



Microfluidic dual picoinjection based encapsulation of hemoglobin in alginate microcapsules reinforced by a poly(l-lysine)-g-poly(ethylene glycol)

Received 00th January 20xx,
Accepted 00th January 20xx

DOI: 10.1039/x0xx00000x

Husnain Ahmed^a, Essa Ahsan Khan^{b,1} and Bjørn Torger Stokke^{a*}

Hemoglobin (Hb) encapsulation inside polysaccharide hydrogels has been considered a possible red blood cell (RBC) surrogate in transfusiology. Here we report on the microfluidic dual picoinjection assisted synthesis of Hb encapsulated alginate-poly(l-lysine)-g-poly(ethylene glycol) beads. This process is realized by the on-chip injections of blended Hb alginate solutions in emulsified aqueous calcium chloride (CaCl₂) droplets followed by a subsequent injection of an aqueous PLL-g-PEG into each emulsified aqueous droplet. The proposed fabrication approach was realized using a flow-focusing and two picoinjection sites in a single PDMS device. Aqueous CaCl₂ solution was emulsified and infused with Hb-alginate solution as the squeezed droplet passed through the first picoinjection site. The injection of PLL-g-PEG to reinforce the microgel and minimize the protein leaching was realized in the second picoinjection site located downstream from the first in the same microfluidic channel. In this process, monodisperse Hb-alginate-PLL-g-PEG particles with a diameter around the size of RBCs (9 μm) were obtained with around 80% of the 7.5 mg/ml Hb included in the injected aqueous alginate retaining in the obtained microparticles. Microparticles with Hb loading (32.8 pg/bead) and retention (28.8 pg/bead) over a week of storage at 4 °C are in accordance with the average amount of Hb per RBC. The Hb-alginate-PLL-g-PEG microbeads fabricated in the size range of RBCs are significant for further exploration

Introduction

Blood transfusion is a vital lifesaving therapy during a traumatic hemorrhage injury or in surgical operations and is also significant in remote civilian areas and under severe battlefield conditions.^{1–4} There is, however, limited availability of healthy blood donors compared to the demands for various blood transfusions. Additionally, existing issues related to the transfusion of human blood, such as limited shelf life (42 days) and requirements for specific storage conditions, may limit blood availability under medical emergencies at point-of-injury locations in the military and civilian fields.^{5–8} Other limitations include possible viral contamination such as HIV or hepatitis, the necessity of cross-matching between donor and receptors, and blood aging that can significantly decrease the efficacy of blood transfusion. Overall, this may lead to adverse effects such as febrile non-hemolytic transfusion in addition to acute lung injury and simple allergic reaction.^{9,10}

The challenges alluded to above can be addressed by developing a synthetic substitute of the blood components manufactured in vitro for sufficient availability across the globe. Synthetic blood substitutes may also be sterilized to reduce the risk of infectious diseases associated with the transfusion. Blood surrogates can be designed with longer shelf life, even outside hospitals, that offer possibilities for on-demand administration to patients in emergencies. Moreover, the immunogenic risk can be reduced due to the lack of need for type matching as the blood substitutes belong to the universal blood group O negative.^{11–13} A substantial body of research has been conducted over the past several decades to discover human blood substitute products that have also extended toward preclinical and clinical assessments.^{14–20} Despite continued exploration, to date, there is no clinically approved product (Hemoglobin-based oxygen carriers or Perfluorocarbons) by Food and Drug Administration available for human applications in the United States.^{14,16} Certain oxygen therapeutics are approved, hemopure for human use in South Africa and oxyglogin for veterinary medicine in Europe and the United States. Nevertheless, a meta-analysis of 16 clinical trials of five different RBC substitutes administered to 3500 patients suggested a threefold increase in the risk of heart attacks and death compared to the controlled group treated with human blood.²¹

The blood substitute has to satisfy the hemoglobin (Hb) functionality by being able to carry oxygen (O₂) from the lungs

^a Biophysics and Medical Technology, Dept. of Physics, NTNU, Norwegian University of Science and Technology, NO-7491 Trondheim, Norway. E-mail: bjorn.stokke@ntnu.no

^b Dept. of Biology, NTNU, Trondheim, Norway

¹ Current affiliation: Dept. of Biotechnology and Food Science, NTNU, Trondheim, Norway

Electronic Supplementary Information (ESI) available: Additional schematic, results, and experimental details. See DOI: 10.1039/x0xx00000x

to other body parts. However, the pure Hb injected into the human body without the red blood cells (RBCs) wrapping is reported to cause blood vessels to tighten with a concomitant increase in blood pressure, heart attack, a cascading line of incidents which eventually can be fatal.^{22,23}

Hemoglobin-based oxygen carriers (HBOCs) prepared using a chemical modification of Hb like polymerization, crosslinking, and macromeric surface conjugations have also been suggested.^{24–26} However, serious adverse effects such as various degrees of deterioration in kidney function, organ damage, neurotoxicity, and increased mortality have been observed in their clinical trials. Therefore stopped using these approaches in clinical transformation.^{18,27,28}

In parallel to the chemically modified HBOCs, there has been some advancement in encapsulation of Hb within various micro- and nano-carrier entities, a strategy that more closely mimics the natural encapsulation of Hb existing in RBCs.¹⁹ An example of this technology is Hb-encapsulated within PEG-ylated liposomal vesicles (HbV).^{29,30} The individual HbV vesicle diameter of 250 nm contains 30,000 Hb molecules. However, this HbV vesicle preparation route possesses challenges related to the broad vesicle size distribution and batch-to-batch variations in the efficiency of the Hb encapsulation.¹⁹ In addition to the strategies for Hb immobilization in lipid vesicles, Hb encapsulated into biocompatible micro and nanoparticles prepared from polymers such as PEG-PLA, PCL (poly ϵ -caprolactone)/PLA co-polymers, PLL (poly(L-lysine)), and PLGA (Poly lactic-co-glycolic acid)/PEG co-polymers, are reported.^{31–33} In another approach, Hb was entrapped in microparticles by its coprecipitations with calcium carbonate (CaCO_3), subsequent crosslinking by glutaraldehyde, and selective dissolution of CaCO_3 , resulting in Hb microparticles with Hb quantity close to that of RBCs.³⁴ Although high Hb content has been achieved in suspensions of the materials prepared in these approaches, the overall functionality as an

oxygen carrier substitute, e.g. including combination of requirements on stability, rheological and circulation life time, assessment of hematological risks, were not demonstrated.

Alginates, a family of natural brown algae polysaccharides, are also utilized to encapsulate various bioactive agents such as proteins, enzymes, cells, antibodies, and DNA due to their mild gelation conditions and biocompatibility, and non-toxic nature.^{35–37} For instance, the Hb was encapsulated in calcium alginate beads using ionotropic gelation for the sol-gel transition of the matrix. This was conducted by dripping the blend of Hb and sodium alginate solution into the excess of aqueous solutions of crosslinking ions (Ca^{2+}), where the resulting beads subsequently were coated using a cationic polysaccharide (chitosan) to limit the leaching of encapsulated protein. Storage conditions and Hb release at different pH have been investigated.³⁸ The employed process yielded the size of the resulting beads of 1000 μm . In another study, Hb was encapsulated inside chitosan-coated alginate microspheres by emulsification/internal gelation technique. This process resulted in the agglomeration of most of the particles in addition to the large size distribution.^{39,40} In yet another approach, alginate-poly(L-histidine) microcapsules were manufactured by ionotropic gelation, and Hb was loaded by the absorption method following the microcapsule formation.⁴¹ The size of the produced bead was $>300 \mu\text{m}$. The drug loading, protein retention, and *in vitro* release characteristics were studied. The size of the entities used to immobilize Hb in the above-summarized studies being 50 – 100 times larger than the typical size $\sim 8 \mu\text{m}$ of natural RBC severely limits their possible clinical applications.

In the present study, we address the challenge associated with the rather large size of the resulting beads in the immobilization process of Hb as a proof-of-concept process for artificial oxygen carriers. The aqueous droplet with Ca^{2+} is injected with a blend of alginate and Hb in the first injection site,

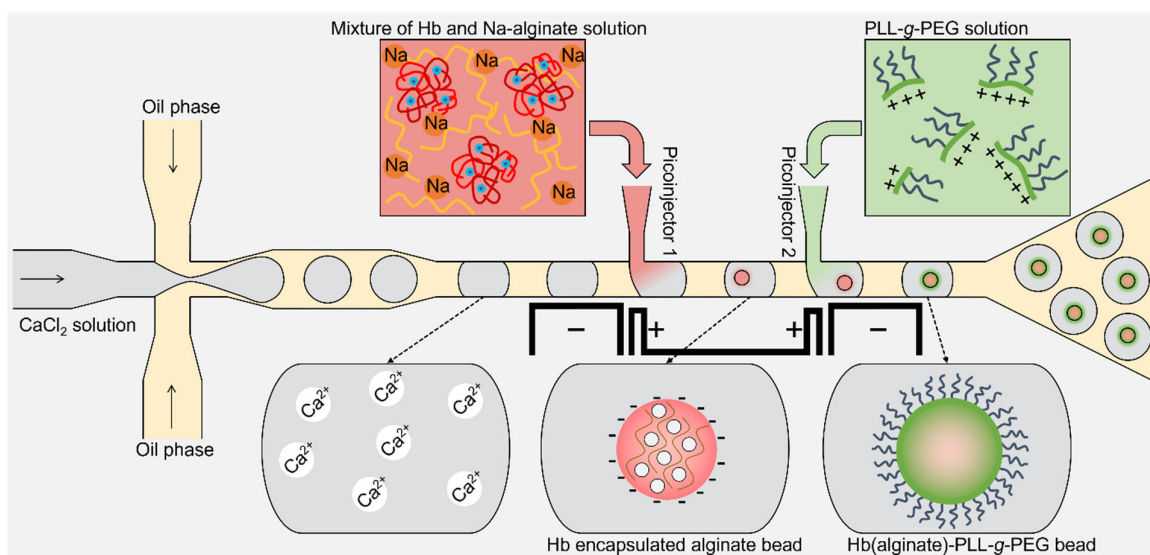


Fig. 1 Schematic illustration of Hb-loaded alginate-PLL-g-PEG synthesis by the picoinjection of the aqueous mixture of Na-alginate and Hb into an aqueous CaCl_2 droplet from picoinjector 1 followed by the injection of PLL-g-PEG from picoinjector 2. The homogenous-sized populations of ionically crosslinked alginate containing Hb were reinforced with cationic polymer exploiting an electrostatic mechanism.

thus resulting in Ca-induced crosslinking mediated by the ionotropic gelation. The electrode adjacent to the T-junction of the picoinjector sites sets up an AC electrical potential as needed to induce coalescence of the surfactant stabilized aqueous droplets.^{42–44} These aqueous droplets are in the same process line, passing the second picoinjection site where an aqueous solution of PLL-*g*-PEG is added to reinforce the Hb-alginate gel beads. The comb-like branched PLL-*g*-PEG was selected as the reinforcing compound due to its dual functionality where the positive charged PLL backbone are envisioned to mediate the anchoring to the alginate matrix by an electrostatic mechanism analogous to that in polyelectrolyte multilayer and complex formation. The grafted PEG chains on PLL are intended serve to reduce possible agglomeration of the resulting microparticles when transferred to an aqueous solution.^{45–47} The resulting Hb-alginate gel beads were extracted from the emulsion state and characterized with respect to Hb encapsulation efficiency and leaching during subsequent storage.

Experimental Section

Device fabrication

A dual picoinjection device was fabricated using a single-layered PDMS microchannel attached to a glass slide, followed by the injection of low melting temperature solder into the tailor-made microchannels for electrodes. The electrode material (Indalloy #19 – 51IN, 32BI, 16.5SN) was introduced into the microfluidic devices by placing the device and a piece of indium alloy in the Eppendorf tube on a hotplate at 95 °C. The melted solder was injected into the custom-designed channel. The device was removed from the hotplate after connecting the electrodes with a metal connector (RND 205-00203, male header, Elfa Distrelec) as described previously.⁴⁸ The commonly used soft lithography processes were used to fabricate the custom-designed PDMS microchannel (Fig. S1). Briefly, a negative photoresist (mr DWL-40) was spin-coated onto the silicon wafer to the desired layer thickness and patterned using a direct laser writing tool (MLA 150), followed by the removal of the unexposed photoresist using a developer (mr-Dev 600). The resulting pattern acted as a mold for the microchannel onto which the PDMS (blended base and curing agent Sylgard 184A and 185B, Dow Corning, (10:1)) was poured. The casted PDMS was cured (65 °C, 4 hours), peeled off from the master and inlet and outlet holes punched through the peeled-off microchannel using a 1 mm punching tool (Harris Uni-core) for flow focusing/droplet generation, picoinjection, and emulsion collection, while 2 mm puncher for electrode channels. Finally, the microchannel was bonded to the microscope slide using oxygen plasma bonding. The width and height of the fabricated microchannels were 25 and 35 μm, respectively. The surface of the fabricated microfluidic channel was rendered hydrophobic by fill-up of the fluorinated oil (Pico-Wave 7500, Sphere Fluidics) containing 2% (v/v) fluorosilane (1H,1H,2H,2H-perfluorooctyl) before the operation of the droplet generation and picoinjection device.

Solutions preparation

The mixture of hemoglobin and alginate solution was prepared by dissolving lyophilized powdered human hemoglobin (Sigma-Aldrich) and powdered sodium alginate (PRONOVA UP LVM) in aqueous bicarbonate buffer (50 mM, pH 9.6, Sigma). All aqueous solutions were prepared using de-ionized water (Resistivity 18.2 MΩ cm, Milli-Q, Merck). The final weight of the alginate in the 1 ml of prepared solution was 10 mg, while the hemoglobin was added to 4 different concentrations: 7.5 mg/ml, 10mg/ml, 15mg/ml, and 20 mg/ml. The solution of cationic polymer PLL(20kDa)-grafted(3.5)-PEG(5kDa) (Surface technology – Susos) and tetramethylrhodamine labeled PLL(20kDa)-grafted(3.5)-PEG(2kDa) (Surface technology – Susos) were prepared by dissolving the co-polymer in phosphate-buffered saline (137mM NaCl, 2.7mM KCl, 10mM phosphate buffer, pH7.4, VWR) to the desired concentration (0.5 mg/ml) of the stock solution. The crosslinking ion solution was prepared by dissolving CaCl₂·2H₂O salt (7.35 mg/ml) in de-ionized water that also contains 27.3 mg/ml mannitol to reduce the effect of change in local osmolarity associated with the ionotropic gelation.⁴⁸ The pH of the solution was adjusted to 7.0 using sodium hydroxide. The tris buffer (2-amino-2-(hydroxymethyl)-1,3 propanediol, Sigma-Aldrich) was prepared by dissolving the powdered tris in de-ionized water (50 mM) that contains 2.35mM CaCl₂. The Bradford reagent was prepared by adding 81 mg SERVA blue G (Acid Blue 90, COOMASSIE® Brilliant Blue G-250, Xylene Brilliant Cyanine G) and 100 ml of 96% ethanol to the total volume of 1000 ml. The reagent was mixed with the 17% phosphoric acid in equal volumes before use. All the solutions were filtered using 200 nm pore size (4483T, Pall Corporation) to remove undissolved residue prior to use.

Experimental setup

The custom-fabricated microfluidic device for drop generation and subsequent dual pico-injections was placed on the inverted microscope (Nikon eclipse Ti2) XY-adjustable stage for visualization of the ongoing experiment (using 10×, 15×, 20×, 30×, 40×, or 60× magnification). The inlets of the microchannel were connected with four syringe pumps (NEMESYS, Cetoni GmbH, Germany; Harvard Apparatus, PHD ULTRA) using microtubing (PE/2, Scientific Commodities) to control the process parameters. Three syringe pumps were used for independent control of the volumetric flow rates of the aqueous phases and one for the oil phase (Pico-Surf™ 1, 2% (w/w) in Novec™ 7500, Sphere Fluidics). The on-chip electrodes were connected to a high voltage amplifier (623B, TREK) through copper wires connected to a metal connector (RND 205-00181, female header, Elfa Distrelec). The high voltage amplifier amplified the signal provided by a waveform generator (33600A, Keysight) before feeding to the on-chip electrodes (200 Vp-p, 30kHz). A high-speed camera (FASTCAM SA3, Photron, model: 120 K M1) attached to the microscope was employed to monitor the flow and pico-injection processes. The oil and surfactant were removed from the collected aqueous droplets following the protocol set by the emulsion-

breaking solution (Pico-Break 1, Sphere Fluidics). A spectrophotometer (Cytation 5, BioTek) was used to measure the optical density of the supernatant solution at 400 nm utilizing a Hemoglobin Assay Kit (MAK115, Sigma-Aldrich) to quantify the amount of Hb loaded in the microgel beads. A Bradford assay was used to visualize the presence of Hb inside alginate-PLL-*g*-PEG particles. The Hb-alginate-PLL-*g*-PEG entities were analyzed by using various microscopes: confocal microscope (LEICA TCS SP8, 40× objective, and appropriate filters for the fluorescently labeled PEG), inverted microscope with a fluorescent camera (Nikon D-LED1), and color camera (Nikon digital sight) using 20× and 40× magnification. The captured microscopic images were processed using an image processing software, ImageJ (<http://imagej.nih.gov/ij/>). The sizes (S) of the bead were obtained as an equivalent diameter of a spherical shape with the same area as the experimental one, calculated using the following relation

$$S = 2\sqrt{A/\pi}$$

where A is the projected area of the Hb-alginate bead obtained by the image processing (ImageJ). The circularity (C) was calculated using the computed area A and perimeter P in the following relation

$$C = 4\pi A/P^2$$

Fabrication of Hb-loaded alginate-PLL-*g*-PEG microcapsules

The Hb-encapsulated microgel beads reinforced with PLL-*g*-PEG were fabricated by employing a microfluidic droplet generation device with integrated dual picoinjection sites and a separate set of channels filled with material supporting the generation of an electric field in the proximity of the picoinjection sites. Firstly, the device emulsified the aqueous CaCl₂ to homogeneously sized droplets in the oil phase using flow-focusing. The aqueous CaCl₂ droplets were subsequently squeezed downstream to the picoinjection sites. In the picoinjector 1, a mixture of Hb and Na-alginate solution was injected into each emulsion droplet and further transported to the picoinjector 2, where the solution of the cationic polymer

was injected into the droplet containing Hb-alginate bead to minimize the leakage of the Hb from the microgel by the interaction between anionic alginate and cationic polymer. The used PLL-*g*-PEG exploits an electrostatic mechanism of the PLL backbone interacting with the alginate gel bead and at the same time yields PEG brushes on the surface to reduce the likelihood of subsequent agglomeration of the beads. Note that the process of making emulsions, injections of the fluid from both the injectors, and collection of the picoinjected droplets is continuous. The emulsion collected at the outlet was destabilized, and oil was removed. The flow rate of the solution at Picoinjector 1 mainly controls the size of the resultant Hb-loaded alginate bead and the concentration of the PLL-*g*-PEG complexed with Hb-alginate particle is controlled by the flow rate of Picoinjector 2 in addition to the initial concentration of the stock solution.

Results and discussion

Production of Hb-encapsulated Ca-alginate-PLL-*g*-PEG beads

The Hb was encapsulated inside homogeneously sized Ca-alginate beads complexed with PLL-*g*-PEG using consecutive processes realized on the same microfluidic device (Fig. 2(a)). The monodisperse droplets of aqueous 50 mM CaCl₂ solution produced by the flow-focusing region of the device at the rate of ~850 Hz were subsequently electrocoalesced with the blend of aqueous 2% Hb and 1% Na alginate from the picoinjection channel followed by another injection of 0.05% PLL-*g*-PEG solution. The blue, yellow, and red arrows respectively depict an emulsified aqueous CaCl₂ droplet before, and after the picoinjection sites. The flow rate of the oil phase and CaCl₂ solution were 500 μl/hr and 100 μl/hr, respectively. The flow rate of the first picoinjection was 8 μl/hr. These flow rates and the dimensions of the microfluidic channels were selected from the previously reported parametric study to target size of resulting microcapsules close to that of RBC.⁴⁸

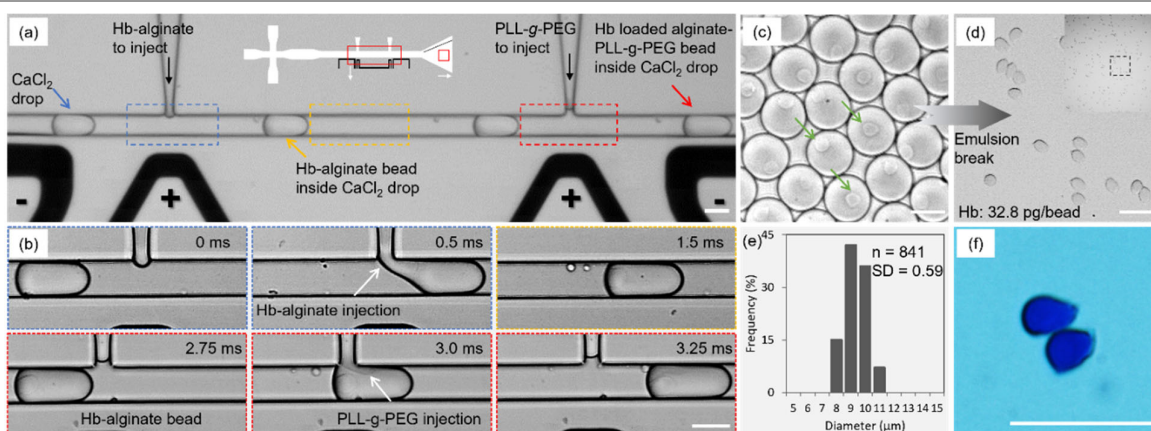


Fig. 2 One-step production of monodisperse Hb-alginate beads. (a) Experimental image of the microfluidic dual picoinjection device used to fabricate Hb carrying alginate gel beads reinforced with co-polymer (PLL-*g*-PEG). (b) Optical micrographs of the time sequence of both the injection steps. The gelation of Hb-alginate and its interaction with PLL-*g*-PEG were initiated by the electrocoalescence of the adjacent droplets in the electric field set up using the adjacent electrodes. The whole process was completed in 3.25 ms. (c,d) Optical micrographs of the Hb-alginate particles before and after the emulsion break of the CaCl₂ droplets show the homogeneous size of the beads. (e) Size distribution of Hb-loaded alginate beads. (f) Optical micrograph of the produced beads suspended in Bradford reagents. This micrograph indicates the presence of Hb inside the polymer beads. All scale bars are 25 μm.

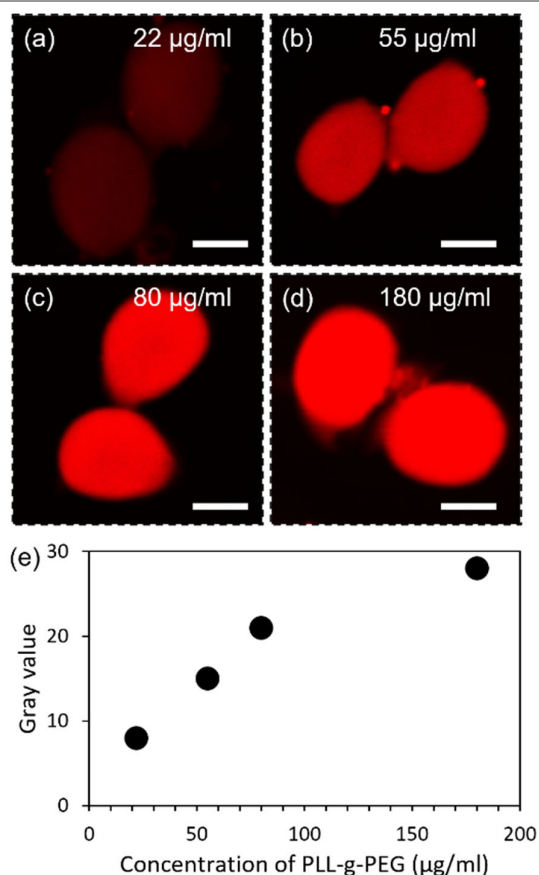


Fig. 3(a) Fluorescent labeled Ca-alginate-PLL-g-PEG beads were prepared with various concentrations of the cationic polymer inside the CaCl_2 droplet after picoinjector 2. (e) The gray value of the produced beads increases from 8 to 28 as the final concentration of the PLL-g-PEG inside the CaCl_2 droplet containing the alginate bead increases from 22 to 180 $\mu\text{g/ml}$. All scale bars are 5 μm .

The flow rate of the second picoinjection was 12 $\mu\text{l/hr}$ that resulted in a concentration of $\sim 55 \mu\text{g/ml}$ of PLL-g-PEG in the droplet when an initial concentration of 500 $\mu\text{g/ml}$ was used. The gelation of Hb-alginate pre-gel solution was initiated by injection into an aqueous droplet of Ca^{2+} completed in around 0.5 ms. The PLL-g-PEG injection was accomplished in 0.5 ms per droplet, which led to the reinforcement of the alginate beads. The residence time between the picoinjection sites of 2.25 ms for the actual devices and flow rates, as stated, proved sufficient duration for maturation of the gel state before the cationic polymer was presented (Fig. 2(b)). Note that in the preliminary experiments, a residence time of around 1 ms for device height 25 μm and specific flow rates of flow-focusing junction (500 $\mu\text{l/hr}$ oil phase and 100 $\mu\text{l/hr}$ CaCl_2 solution) resulted in agglomeration of the beads due to the interaction of the cationic polymer with the anionic alginate bead before its sufficient maturation that interfered with the Ca^{2+} induced crosslinking process.

After the picoinjection sites, the droplets were further transported to the collection domain (Fig. 2(c)). The green arrows show the suspended Hb-polymer bead inside each CaCl_2 drop. Fig. 2(d) shows the bright-field images of the final beads

after the subsequent emulsion break (oil and surfactant removal) and the corresponding size distribution histogram (Fig. 2(e)). The average size and circularity of the produced Hb-loaded alginate-PLL-g-PEG particles are $9 \pm 0.59 \mu\text{m}$ and 0.87 ($n=841$), respectively. The low relative standard deviation indicates the monodispersity of the samples. Moreover, the average amount of the Hb entrapped inside the beads was $\sim 32.8 \text{ pg/bead}$, which corresponds to the mean corpuscular Hb (MCH: 27-31pg). A bright-field image of the beads in the Bradford assay showing blue color further verified the presence of protein inside the beads (Fig. 2(f)).

The injection of the Hb-alginate solution inside the CaCl_2 emulsion also resulted in small satellite droplets due to the relatively high viscosity of the injected solution, which resists the complete break-up of the injected solution. A similar formation of satellite droplets has also been reported for droplet generation in a T-junction device.⁴⁹ These non-crosslinked Hb-alginate droplets were successfully sorted at the collection outlet (Fig. S2) by size-dependent fractionation.⁵⁰

Characterization of on-chip microgel beads interaction with PLL-g-PEG

The process parameter for the concentration of PLL-g-PEG injected into the aqueous emulsified droplets containing alginate microgel was determined by adjusting the injection flow rate and concentration. The flow rates of the continuous (Q_C), dispersed phase (Q_D), and alginate picoinjection (Q_{P1}) were fixed. In contrast, the flow rate of cationic polymer injection (Q_{P2}) and initial concentration of the PLL-g-PEG were varied to obtain various concentrations inside the CaCl_2 drop available to interact with the microgel bead. The PLL backbone interacts electrostatically with the alginate bead, and there is a polymeric brush formed by the side chains (PEG) extending from the PLL backbone. A fluorescent-labeled PLL-g-PEG with the initial concentration of either 250, 500, or 1000 $\mu\text{g/ml}$ was injected ($Q_{P2} = 12 \mu\text{l/hr}$) inside the aqueous CaCl_2 drop carrying a microgel bead, resulting in final concentrations of 22 (Fig. 3(a)), 55 (Fig. 3(b)), and 80 $\mu\text{g/ml}$, respectively (Fig. 3(c)). Moreover, 1000 $\mu\text{g/ml}$ of PLL-g-PEG injected at Q_{P2} of 24 $\mu\text{l/hr}$ resulted in 180 $\mu\text{g/ml}$ of PLL-g-PEG inside the emulsion (Fig. 3(d)). These samples were collected at the outlet, and the resulting distribution of fluorescence intensity was obtained using a CLSM microscope. The increase in the concentration of the grafted co-polymer from 22 to 180 $\mu\text{g/ml}$ in the emulsified droplet resulted in an increase of corresponding gray values up to 80 $\mu\text{g/ml}$ followed by indication of levelling off for further increase (Fig 3(e)). This data indicates increase and subsequent saturation of amount of PLL-g-PEG bound to the alginate gel beads that was used to select the concentration to be used in the further process. In specific, a PLL-g-PEG concentration of 55 $\mu\text{g/ml}$ was used in the further process to keep it lower than 80 $\mu\text{g/ml}$ thus reducing possible unbound PLL-g-PEG in the solution. Injection of the polycation for reinforcement in the individual emulsified droplet containing one microgel bead ensured the realization of the reinforcement process while avoiding the agglomeration of the beads. The interaction of the aqueous cationic polymer with anionic polymer beads off-chip

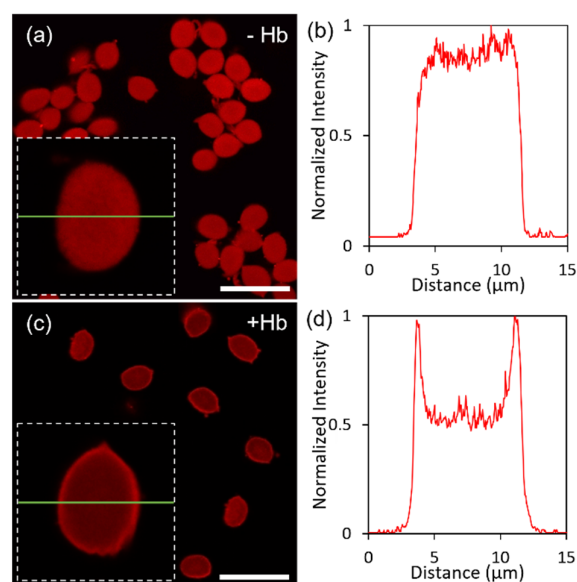


Fig. 4(a) The CLSM fluorescent micrographs of the alginate-PLL-g-PEG particle inside an aqueous medium. **(b)** The intensity profile across the equatorial microbead cross-section shows the distribution of PLL-g-PEG inside the bead shown in the inset of (a). **(c)** The CLSM fluorescent micrographs of the Hb- alginate-PLL-g-PEG bead inside an aqueous medium and corresponding **(d)** intensity profile across the cross-section of the bead shows the distribution of the cationic polymer inside the bead. All scale bars, 25 μm.

also initially explored was observed to induce colonies of polymer complexes and bead agglomeration as observed in the bulk coating of the Hb-loaded alginate beads by the positively charged chitosan.^{39,40}

However, the proposed method offers the generation and strengthening of the microgel beads within the same process realized on one chip, a one-step procedure. This is considered advantageous since the combined reinforcement–coating step at the single microgel particle level reduces the likelihood of polymer-induced bridging in the process.

The distribution of the cationic polymer in the alginate bead (with and without the encapsulation of Hb) was determined using CLSM. The interaction of alginate microgel not loaded with Hb with the fluorescently labeled cationic polymer resulted in the homogenous distribution of the PLL-g-PEG (Fig. 4(a)) as indicated by the fluorescence intensity profile through the cross-section of the alginate-PLL-g-PEG bead (Fig. 4(b)). However, the Ca²⁺ induced crosslinking of the aqueous mixture of Hb and alginate followed by the injection of cationic polymer resulted in a coating of the outer surface of the bead with the PLL-g-PEG, similar to a thin shell-like membrane but still with PLL-g-PEG internal in the microgel (Fig. 4(c)). This difference in the distribution of PLL-g-PEG is suggested to arise from the presence of Hb, which reduces the capacity of the PLL-g-PEG to form a homogenous complex with alginate within the bead. The thickness of the outer membrane is ~0.5 μm. The fluorescent intensity profile across the equator of the Hb-alginate-PLL-g-PEG bead further indicates the localization of some cationic polymer inside the Hb-alginate bead (Fig. 4(d)).

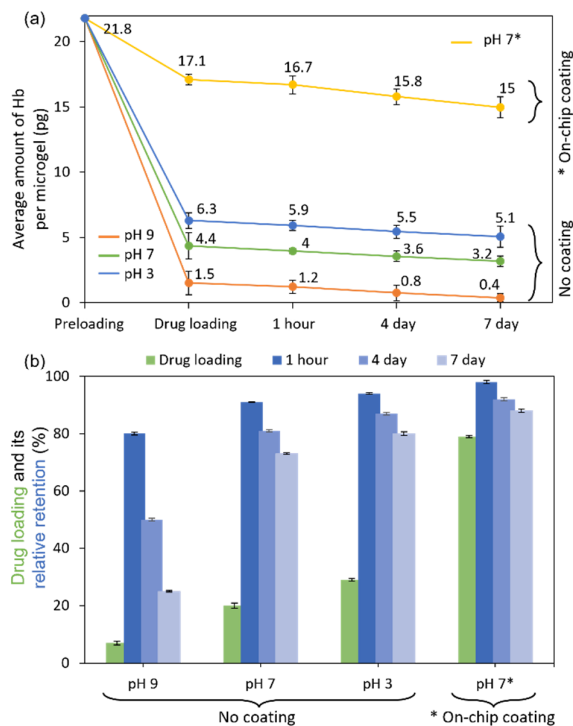


Fig. 5(a) The average amount of Hb-loaded per microgel particle and its retention over 7 days increases significantly as the Hb-alginate beads were coated with cationic polymer on-chip, also with the change in pH of the crosslinking ions solution. **(b)** The percentage of drug loading and its relative retention inside beads prepared with and without on-chip coating method at different pH of crosslinker. The error bars represent the uncertainty in the optical density measurement of the supernatant solution.

Characterization of Hb-loading and protein retention of polymer microbeads

The Hb(drug) was loaded into the microgel bead by premixing with an aqueous alginate solution and crosslinking with Ca²⁺. A microfluidic (flow-focusing with subsequent single picoinjection) device was used to fabricate Hb-alginate beads (without the coating of cationic polymer) by the picoinjection of the mixture of Na-alginate and Hb solution inside CaCl₂ emulsified droplets. Flow rates Q_C and Q_D were 500 and 100 μl/hr, respectively. The Q_{p1} (alginate Hb picoinjection flow rate) of 8 μl/hr resulted in a Hb-alginate bead with an average diameter of 9 μm.

The Hb loading was determined by measuring the non-encapsulated Hb in the supernatant solution (CaCl₂). The microbeads were then transferred into Tris buffer after centrifuging and removing the supernatant solution using micropipette, followed by its storage at 4 °C. The leaching of Hb from the polymer beads was quantified over time by measuring the leaked Hb in the supernatant solution (tris buffer). The drug loading and relative protein retention were calculated by using the following relations

$$\text{Drug loading (\%)} = \frac{\alpha_1 - \beta_1}{\alpha_1}$$

$$\text{Relative protein retention (\%)} = \frac{\alpha_2 - \beta_1}{\alpha_2}$$

where α_1 is the total weight of the Hb used for encapsulation, α_2 is the encapsulated weight of the Hb inside microbeads and β_1 is the weight of the leaked Hb in the supernatant solution calculated by measuring its optical density.

Using 0.75% Hb, 1% alginate, and CaCl₂ solution of pH 9 resulted in 1.5 pg Hb per bead corresponding to 7% drug loading. A substantial decline in the relative protein retention was observed over time—80 (1.2 pg/bead), 50 (0.8 pg/bead), and 25% (0.4 pg/bead) determined after 1 hour, 4 days, and 7 days storage at 4 °C, respectively. Using a lower pH of the crosslinking solution increased the drug loading and decreased the Hb leaching. At pH 7 and 3, the drug loading was increased to 20 (4.4 pg/bead) and 29% (6.3 pg/bead), respectively. The average Hb per bead was decreased from 4.4 to 3.2 pg and 6.3 to 5.1 pg, which corresponds to a decrease in relative protein retention to 73 and 80% after 7 days of storage. The trends in the effect of pH and coating on the amount of Hb loaded per microgel and leaching during storage can be visualized in Fig. 5(a). The drug loading and relative protein retention percentage are presented in Fig. 5(b).

An even lower Hb-loading and faster leaching were observed when the microgels were not reinforced with a cationic polymer. The Hb inside the alginate microgel was found to leach, possibly arising from the porous sizes of the gel. Therefore, the coating of the microgel with cationic polymer on-chip was indispensable. The pH of the emulsified droplets was fixed to 7 during the synthesis of the Hb-alginate bead and subsequent coating with the PLL-*g*-PEG to keep the physiological condition for Hb and favorable condition for the cationic polymer to react with the microgel electrostatically. The one-by-one on-chip coating of the Hb-alginate beads increased the amount of Hb loaded per microgel nearly fourfold (4.4 to 17.1 pg), corresponding to an increase in the drug loading from 20 to 79% when compared with the microbeads prepared without the protective coating. The Hb leaching also decreased drastically during storage in tris buffer. The relative protein retention was 98, 92, and 88% analyzed after 1 hour, 4 hours, and 7 days, corresponding to 16.7, 15.8, and 15 pg of Hb remaining intact with a polymer bead.

After characterizing the fabrication of Hb-loaded alginate-PLL-*g*-PEG microcapsules, the concentration of the Hb in alginate solution was varied (Fig. 6(a)). As the initial concentration of Hb increased from 0.75 to 1%, the drug loading decreased from 79 to 70%. However, the average amount of Hb loaded inside a polymer bead increased from 17.1 to 20 pg—that amount decreased to 19.5, 18.5, and 17.7 pg; per bead evaluated following 1 hour, 4 hours, and 7 days storage, respectively. Further increase in the Hb concentration (1.5%) in the solution mixture resulted in a further increase of intact Hb inside the bead (27.2 pg) just following completion of the fabrication, which decreased to 23 pg after a week of storage. The percentage of drug loading was decreased to 64%. Using a Hb concentration of 2% further reduced the drug loading to 57%. Nevertheless, the encapsulated amount of Hb increased significantly to 32.8 pg per bead of the PLL-*g*-PEG reinforced Hb-alginate preparation. Minimal leaching was observed during storage at 4 °C—readings were taken after 1 hour, 4 hours, and

7 days of beads preparation, showing the final amount of encapsulated Hb, 32.5, 30.5, and 28.8 pg/bead, respectively.

The intact Hb inside the alginate-PLL-*g*-PEG beads was further verified using the Bradford protein test. Coomassie dye binds to the protein under acidic conditions and exhibits a blue color that verifies the presence of protein. The beads prepared with a 2% initial concentration of Hb after storage for more than a week underwent a qualitative test. Fig. 6(b)) shows the fluorescent image of the Hb-loaded alginate-PLL-*g*-PEG beads with a corresponding bright-field image showing the presence of blue-colored beads, further validating the presence of Hb inside the alginate-PLL-*g*-PEG beads (Fig. 6(c)).

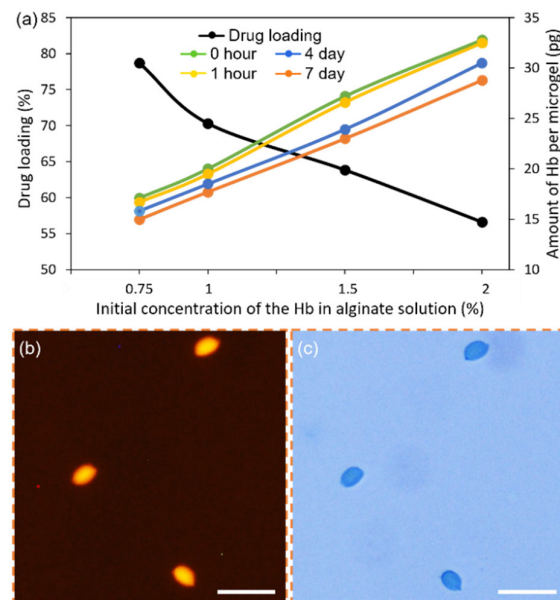


Fig. 6(a) The drug loading percentage and the average amount of Hb per microgel over 7 days versus the initial concentration of the Hb in alginate solution. (b, c) The fluorescence and bright field image of the Hb-alginate-PLL-*g*-PEG beads. Scale bars, 25 μ m.

Performance of suggested fabrication route and resulting Hb loaded microparticles

The suggested fabrication route to achieve Hb-loaded alginate microparticles with a size comparable to the overall dimensions of RBC comes with both challenges as well as opportunities. A particular challenge in the workflow resides in the relatively low throughput (e.g., in the range of beads/min) as governed by the need for consecutive picoinjectors as realized by soft lithography-based approaches. Although the realized device design is not readily scalable, other approaches for microfluidic multiplex designs and fabrication routes^{51–54} can be used as a potential basis for relaxing the high throughput limitation of the design used here.

Using the obtained Hb content in the beads of 32.2 pg/bead and 28.8 pg/bead, obtained as initially loaded after isolation from the emulsion and following storage for one week, respectively, correspond to a Hb content of 4.3 g/dL and 3.8 g/dL for a suspension of the obtained microparticle beads at an assumed volume fraction of 50%. This is nearly up to the 5.2 g/dL

reported for 40% volume fraction suspension of RBC mimicking polymer particles conjugated with Hb.⁵⁵ Although the Hb concentration is lower than the normal physiological range (around 16 g/dL), the obtained Hb content in the present workflow is in the same range as the Hb content of 4.2 g/dL reported for Hb conjugated to PEG of the MP4 oxygen carrier product.⁵⁶

Further development of our proof-of-concept process to develop a RBC substitute should expand on the stability of the components beyond the one-week initial tests included here and tuning of mechanical properties to accommodate rheological properties mimicking whole blood^{57,58} and support of circulation times as well as testing of biocompatible properties. More specific, the Ca-alginate materials are obtainable with different mechanical moduli by the selection of alginate molecular mass, alginate type, and concentration, as well as the concentration of Ca²⁺.^{59–61} The reported parameter space available for tuning the mechanical properties of alginate gels, both in bulk and microgel states, is considered an interesting basis to explore for further developing the current workflow for Hb-alginate microparticles with respect to mechanical properties.

Conclusions

In the present paper, we have described the inclusion of Hb in the process of a novel picoinjection-based microfluidic platform for the production of chelate free Ca-alginate beads and their subsequent reinforcement by a comb-like branched polycation to reduce Hb leaching from the resulting beads. The process exploits electrocoalescence in the picoinjection sites, and despite the induction of a sol-gel reaction and polymer associations in both these picoinjection sites, the device is not clogged in the process. This lack of clogging is probably due to the short duration of electrocoalescence-induced droplet merger (less than 0.5 ms) compared to gelation time, as described in more detail previously.⁴⁸ Using this fabrication process, monodisperse Ca-alginate microgel beads with hemoglobin and reinforced with PLL-*g*-PEG were obtained with an average size of 9 μm, which is in the range of RBCs. Moreover, the amount of Hb, tunable by the concentration in the aqueous solution including alginate, could be obtained to a maximum of 32.8 pg/bead. The Hb was retained for this preparation at 28.8 pg/bead over a week of storage at 4 °C. This level of Hb is in the same range as the average amount of Hb per RBC.

While the proof-of-concept and retention studied here are addressing the inclusion of Hb in the microgel beads, it is believed that the designed fabrication strategy also is applicable for immobilization of other components, in particular cases where the included active component may be sensitive to the presence of chelators or non-physiological pH history as needed for other realizations. In such a context, it should also be noted that sizes of microgel beads can be tuned by the combined

tailor-making devices with different microfluidic dimensions and their operation as indicated.⁴⁸

Authors' contributions

H.A. and B.T.S. conceived the research. B.T.S. supervised the research. H.A. designed the experiments. H.A. and E.A.K. performed the experiments. H.A., E.A.K., and B.T.S. contributed to the manuscript preparation. All authors have given approval to the final version of the manuscript.

Conflict of interest

There are no conflicts to declare.

Acknowledgements

This work is supported by the Research Council of Norway, project Norwegian Micro- and Nano-Fabrication Facility, NorFab, project number 245963/F50.

References

- (1) Monkkonen, L.; Edgar, J. S.; Winters, D.; Heron, S. R.; Mackay, C. L.; Masselon, C. D.; Stokes, A. A.; Langridge-Smith, P. R. R.; Goodlett, D. R. Screen-Printed Digital Microfluidics Combined with Surface Acoustic Wave Nebulization for Hydrogen-Deuterium Exchange Measurements. *J. Chromatogr. A* **2016**, *1439*, 161–166.
- (2) Holcomb, J. B.; Tilley, B. C.; Baraniuk, S.; Fox, E. E.; Wade, C. E.; Podbielski, J. M.; Del Junco, D. J.; Brasel, K. J.; Bulger, E. M.; Callcut, R. A.; et al. Transfusion of Plasma, Platelets, and Red Blood Cells in a 1:1:1 vs a 1:1:2 Ratio and Mortality in Patients with Severe Trauma: The PROPPR Randomized Clinical Trial. *JAMA - J. Am. Med. Assoc.* **2015**, *313* (5), 471–482.
- (3) Blackburne, L. H.; Baer, D. G.; Eastridge, B. J.; Kheirabadi, B.; Kragh, J. F.; Cap, A. P.; Dubick, M. A.; Morrison, J. J.; Midwinter, M. J.; Butler, F. K.; et al. Military Medical Revolution: Prehospital Combat Casualty Care. *J. Trauma Acute Care Surg.* **2012**, *73* (6 SUPPL. 5), 372–377.
- (4) Holcomb, J. B.; Jenkins, D.; Rhee, P.; Johannigman, J.; Mahoney, P.; Mehta, S.; Cox, E. D.; Gehrke, M. J.; Beilman, G. J.; Schreiber, M.; et al. Damage Control Resuscitation: Directly Addressing the Early Coagulopathy of Trauma. *J. Trauma - Inj. Infect. Crit. Care* **2007**, *62* (2), 307–310.
- (5) Smith, J. W.; Gilcher, R. O. Red Blood Cells, Plasma, and Other New Apheresis-Derived Blood Products: Improving Product Quality and Donor Utilization. *Transfus. Med. Rev.* **1999**, *13* (2), 118–123.
- (6) Cap, A. P.; Pidcoke, H. F.; De Pasquale, M.; Rappold, J. F.; Glassberg, E.; Eliassen, H. S.; Bjerkvig, C. K.; Fosse, T. K.; Kane, S.; Thompson, P.; et al. Blood Far Forward: Time to Get Moving! *J. Trauma Acute Care Surg.* **2015**, *78* (6), S2–S6.

- (7) Boscarino, C.; Tien, H.; Acker, J.; Callum, J.; Hansen, A. L.; Engels, P.; Glassberg, E.; Nathens, A.; Beckett, A. Feasibility and Transport of Packed Red Blood Cells into Special Forces Operational Conditions. *J. Trauma Acute Care Surg.* **2014**, *76* (4), 1013–1019.
- (8) Spinella, P. C.; Dunne, J.; Beilman, G. J.; O'Connell, R. J.; Borgman, M. A.; Cap, A. P.; Rentas, F. Constant Challenges and Evolution of US Military Transfusion Medicine and Blood Operations in Combat. *Transfusion* **2012**, *52* (5), 1146–1153.
- (9) Blajchman, M. A. Bacterial Contamination and Proliferation during the Storage of Cellular Blood Products. *Vox Sang.* **1998**, *74* (SUPPL. 2), 155–159.
- (10) Seghatchian, J.; de Sousa, G. Pathogen-Reduction Systems for Blood Components: The Current Position and Future Trends. *Transfus. Apher. Sci.* **2006**, *35* (3), 189–196.
- (11) Chang, T. M. S. Blood Substitutes Based on Nanobiotechnology. *Trends Biotechnol.* **2006**, *24* (8), 372–377.
- (12) Squires, J. E. Artificial Blood. *Science (80-.)*. **2002**, *295* (5557).
- (13) Blajchman, M. A. Substitutes for Success. *Nat. Med.* **1999**, *5* (1), 17–18.
- (14) Sen Gupta, A. Hemoglobin-Based Oxygen Carriers: Current State-of-the-Art and Novel Molecules. *Shock* **2019**, *52* (1S), 70–83.
- (15) Buehler, P. W.; D'Agnillo, F.; Schaer, D. J. Hemoglobin-Based Oxygen Carriers: From Mechanisms of Toxicity and Clearance to Rational Drug Design. *Trends Mol. Med.* **2010**, *16* (10), 447–457.
- (16) Bialas, C.; Moser, C.; Sims, C. A. Artificial Oxygen Carriers and Red Blood Cell Substitutes: A Historic Overview and Recent Developments toward Military and Clinical Relevance. *J. Trauma Acute Care Surg.* **2019**, *87* (1S Suppl 1), S48–S58.
- (17) Abbyad, P.; Tharaux, P. L.; Martin, J. L.; Baroud, C. N.; Alexandrou, A. Sickling of Red Blood Cells through Rapid Oxygen Exchange in Microfluidic Drops. *Lab Chip* **2010**, *10* (19), 2505–2512.
- (18) Chang, T. M. S. Future Generations of Red Blood Cell Substitutes. *J. Intern. Med.* **2003**, *253* (5), 527–535.
- (19) Tao, Z.; Ghoroghchian, P. P. Microparticle, Nanoparticle, and Stem Cell-Based Oxygen Carriers as Advanced Blood Substitutes. *Trends Biotechnol.* **2014**, *32* (9), 466–473.
- (20) Winslow, R. M. New Transfusion Strategies: Red Cell Substitutes. *Annu. Rev. Med.* **1999**, *50* (1), 337–353.
- (21) Sauaia, A.; Moore, E. E.; Banerjee, A. Hemoglobin-Based Blood Substitutes and Risk of Myocardial Infarction and Death. *JAMA - J. Am. Med. Assoc.* **2008**, *300* (11), 1297.
- (22) Alayash, A. I. Setbacks in Blood Substitutes Research and Development: A Biochemical Perspective. *Clin. Lab. Med.* **2010**, *30* (2), 381–389.
- (23) Amberson, W. R.; Jennings, J. J.; Rhode, C. M. Clinical Experience with Hemoglobin-Saline Solutions. *J. Appl. Physiol.* **1949**, *1* (7), 469–489.
- (24) Simoni, J.; Simoni, G.; Moeller, J. F.; Feola, M.; Wesson, D. E. Artificial Oxygen Carrier with Pharmacologic Actions of Adenosine-5'-Triphosphate, Adenosine, and Reduced Glutathione Formulated to Treat an Array of Medical Conditions. *Artif. Organs* **2014**, *38* (8), 684–690.
- (25) Jahr, J. S.; Moallempour, M.; Lim, J. C. HBOC-201, Hemoglobin Glutamer-250 (Bovine), Hemopure® (Biopure Corporation). *Expert Opin. Biol. Ther.* **2008**, *8* (9), 1425–1433.
- (26) Cheng, D. C. H.; Mazer, C. D.; Martineau, R.; Ralph-Edwards, A.; Karski, J.; Robblee, J.; Finegan, B.; Hall, R. I.; Latimer, R.; Vuylsteke, A. A Phase II Dose-Response Study of Hemoglobin Raffimer (Hemolink) in Elective Coronary Artery Bypass Surgery. *J. Thorac. Cardiovasc. Surg.* **2004**, *127* (1), 79–86.
- (27) Gould, S. A.; Moore, E. E.; Hoyt, D. B.; Burch, J. M.; Haenel, J. B.; Garcia, J.; DeWoskin, R.; Moss, G. S. The First Randomized Trial of Human Polymerized Hemoglobin as a Blood Substitute in Acute Trauma and Emergent Surgery. *J. Am. Coll. Surg.* **1998**, *187* (2), 113–120.
- (28) Chen, J. Y.; Scerbo, M.; Kramer, G. A Review of Blood Substitutes: Examining the History, Clinical Trial Results, and Ethics of Hemoglobin-Based Oxygen Carriers. *Clinics* **2009**, *64* (8), 803–813.
- (29) Taguchi, K.; Urata, Y.; Anraku, M.; Watanabe, H.; Kadowaki, D.; Sakai, H.; Horinouchi, H.; Kobayashi, K.; Tsuchida, E.; Maruyama, T.; et al. Hemoglobin Vesicles, Polyethylene Glycol (PEG)ylated Liposomes Developed as a Red Blood Cell Substitute, Do Not Induce the Accelerated Blood Clearance Phenomenon in Mice. *Drug Metab. Dispos.* **2009**, *37* (11), 2197–2203.
- (30) Tsuchida, E.; Sou, K.; Nakagawa, A.; Sakai, H.; Komatsu, T.; Kobayashi, K. Artificial Oxygen Carriers, Hemoglobin Vesicles and Albumin-Hemes, Based on Bioconjugate Chemistry. *Bioconjug. Chem.* **2009**, *20* (8), 1419–1440.
- (31) Sheng, Y.; Yuan, Y.; Liu, C.; Tao, X.; Shan, X.; Xu, F. In Vitro Macrophage Uptake and in Vivo Biodistribution of PLA-PEG Nanoparticles Loaded with Hemoglobin as Blood Substitutes: Effect of PEG Content. *J. Mater. Sci. Mater. Med.* **2009**, *20* (9), 1881–1891.
- (32) Chang, T. M. S. Nanobiotechnology for Hemoglobin-Based Blood Substitutes. *Crit. Care Clin.* **2009**, *25* (2), 373–382.
- (33) Rameez, S.; Alost, H.; Palmer, A. F. Biocompatible and Biodegradable Polymersome Encapsulated Hemoglobin: A Potential Oxygen Carrier. *Bioconjug. Chem.* **2008**, *19* (5), 1025–1032.
- (34) Duan, L.; Yan, X.; Wang, A.; Jia, Y.; Li, J. Highly Loaded Hemoglobin Spheres as Promising Artificial Oxygen Carriers. *ACS Nano* **2012**, *6* (8), 6897–6904.
- (35) Lee, K. Y.; Mooney, D. J. Alginate: Properties and Biomedical Applications. *Prog. Polym. Sci.* **2012**, *37* (1), 106–126.
- (36) Sun, J.; Tan, H. Alginate-Based Biomaterials for Regenerative Medicine Applications. *Materials (Basel)*. **2013**, *6* (4), 1285–1309.
- (37) Gombotz, W. R.; Wee, S. F. Protein Release from Alginate Matrices. *Adv. Drug Deliv. Rev.* **1998**, *31* (3), 267–285.
- (38) Huguet, M. L.; Groboillot, A.; Neufeld, R. J.; Poncetlet, D.; Dellacherie, E. Hemoglobin Encapsulation in

- Chitosan/Calcium Alginate Beads. *J. Appl. Polym. Sci.* **1994**, *51* (8), 1427–1432.
- (39) Ribeiro, A. J.; Silva, C.; Ferreira, D.; Veiga, F. Chitosan-Reinforced Alginate Microspheres Obtained through the Emulsification/Internal Gelation Technique. *Eur. J. Pharm. Sci.* **2005**, *25* (1), 31–40.
- (40) Silva, C. M.; Ribeiro, A. J.; Figueiredo, M.; Ferreira, D.; Veiga, F. Microencapsulation of Hemoglobin in Chitosan-Coated Alginate Microspheres Prepared by Emulsification/Internal Gelation. *AAPS J.* **2005**, *7* (4), E903–E913.
- (41) Wang, S. Bin; Xu, F. H.; He, H. S.; Weng, L. J. Novel Alginate-Poly(L-Histidine) Microcapsules as Drug Carriers: In Vitro Protein Release and Short Term Stability. *Macromol. Biosci.* **2005**, *5* (5), 408–414.
- (42) Chabert, M.; Dorfman, K. D.; Viovy, J. L. Droplet Fusion by Alternating Current (AC) Field Electrocoalescence in Microchannels. *Electrophoresis* **2005**, *26* (19), 3706–3715.
- (43) Ahn, K.; Agresti, J.; Chong, H.; Marquez, M.; Weitz, D. A. Electrocoalescence of Drops Synchronized by Size-Dependent Flow in Microfluidic Channels. *Appl. Phys. Lett.* **2006**, *88* (26).
- (44) Hauck, N.; Neuendorf, T. A.; Männel, M. J.; Vogel, L.; Liu, P.; Stündel, E.; Zhang, Y.; Thiele, J. Processing of Fast-Gelling Hydrogel Precursors in Microfluidics by Electrocoalescence of Reactive Species. *Soft Matter* **2021**, *17* (45), 10312–10321.
- (45) Laugel, N.; Betscha, C.; Winterhalter, M.; Voegel, J. C.; Schaaf, P.; Ball, V. Relationship between the Growth Regime of Polyelectrolyte Multilayers and the Polyanion/Polycation Complexation Enthalpy. *J. Phys. Chem. B* **2006**, *110* (39), 19443–19449.
- (46) Bharadwaj, S.; Montazeri, R.; Haynie, D. T. Direct Determination of the Thermodynamics of Polyelectrolyte Complexation and Implications Thereof for Electrostatic Layer-by-Layer Assembly of Multilayer Films. *Langmuir* **2006**, *22* (14), 6093–6101.
- (47) Mascotti, D. P.; Lohman, T. M. Thermodynamic Extent of Counterion Release upon Binding Oligolysines to Single-Stranded Nucleic Acids. *Proc. Natl Acad. Sci. U.S.A.* **1990**, *87*, 3142–3146.
- (48) Ahmed, H.; Stokke, B. T. Fabrication of Monodisperse Alginate Microgel Beads by Microfluidic Picoinjection: A Chelate Free Approach. *Lab Chip* **2021**, *21* (11), 2232–2243.
- (49) Abalde-Cela, S.; Taladriz-Blanco, P.; de Oliveira, M. G.; Abell, C. Droplet Microfluidics for the Highly Controlled Synthesis of Branched Gold Nanoparticles. *Sci. Rep.* **2018**, *8* (1), 2440.
- (50) Mazutis, L.; Griffiths, A. D. Preparation of Monodisperse Emulsions by Hydrodynamic Size Fractionation. *Appl. Phys. Lett.* **2009**, *95* (20), 1–4.
- (51) Amstad, E.; Chemama, M.; Eggersdorfer, M.; Arriaga, L. R.; Brenner, M. P.; Weitz, D. A. Robust Scalable High Throughput Production of Monodisperse Drops. *Lab Chip* **2016**, *16* (21), 4163–4172.
- (52) Håti, A. G.; Szymborski, T. R.; Steinacher, M.; Amstad, E. Production of Monodisperse Drops from Viscous Fluids. *Lab Chip* **2018**, *18* (4), 648–654.
- (53) Wu, J.; Yadavali, S.; Lee, D.; Issadore, D. A. Scaling up the Throughput of Microfluidic Droplet-Based Materials Synthesis: A Review of Recent Progress and Outlook. *Appl. Phys. Rev.* **2021**, *8* (3), 031304.
- (54) Toren, P.; Smolka, M.; Haase, A.; Palfinger, U.; Nees, D.; Ruttloff, S.; Kuna, L.; Schauder, C.; Jauk, S.; Rimpler, M.; et al. High-Throughput Roll-to-Roll Production of Polymer Biochips for Multiplexed DNA Detection in Point-of-Care Diagnostics. *Lab Chip* **2020**, *20* (22), 4106–4117.
- (55) Chen, K.; Merkel, T. J.; Pandya, A.; Napier, M. E.; Luft, J. C.; Daniel, W.; Sheiko, S.; Desimone, J. M. Low Modulus Biomimetic Microgel Particles with High Loading of Hemoglobin. *Biomacromolecules* **2012**, *13* (9), 2748–2759.
- (56) Coll-Satue, C.; Bishnoi, S.; Chen, J.; Hosta-Rigau, L. Stepping Stones to the Future of Haemoglobin-Based Blood Products: Clinical, Preclinical and Innovative Examples. *Biomater. Sci.* **2021**, *9* (4), 1135–1152.
- (57) Merkel, T. J.; Jones, S. W.; Herlihy, K. P.; Kersey, F. R.; Shields, A. R.; Napier, M.; Luft, J. C.; Wu, H.; Zamboni, W. C.; Wang, A. Z.; et al. Using Mechanobiological Mimicry of Red Blood Cells to Extend Circulation Times of Hydrogel Microparticles. *Proc. Natl. Acad. Sci. U. S. A.* **2011**, *108* (2), 586–591.
- (58) Rubio, A.; López, M.; Rodrigues, T.; Campo-Deaño, L.; Vega, E. J. A Particulate Blood Analogue Based on Artificial Viscoelastic Blood Plasma and RBC-like Microparticles at a Concentration Matching the Human Haematocrit. *Soft Matter* **2022**, 7510–7523.
- (59) Draget, K. I.; Stokke, B. T.; Yuguchi, Y.; Urakawa, H.; Kajiwara, K. Small-Angle X-Ray Scattering and Rheological Characterization of Alginate Gels. 3. Alginic Acid Gels. *Biomacromolecules* **2003**, *4* (6), 1661–1668.
- (60) Martinsen, A.; Skjåk-Bræk, G.; Smidsrød, O. Alginate as Immobilization Material: I. Correlation between Chemical and Physical Properties of Alginate Gel Beads. *Biotechnol. Bioeng.* **1989**, *33* (1), 79–89.
- (61) Bassett, D. C.; Håti, A. G.; Melø, T. B.; Stokke, B. T.; Sikorski, P. Competitive Ligand Exchange of Crosslinking Ions for Ionotropic Hydrogel Formation. *J. Mater. Chem. B* **2016**, *4* (37), 6175–6182.